

**Table 2.** Detection limits, RSD(%), and plates of selected steroids with sweeping (12).

Steroids	Progesterone	Testosterone	Fluocinolone	Dexamethasone
Equation of line	$y = 1.27x - 1.58$	$y = 1.18x - 1.34$	$y = 1.00x - 1.32$	$y = 0.89x - 0.98$
Coefficient of variation	$r^2 = 0.9890$	$r^2 = 0.9866$	$r^2 = 0.9859$	$r^2 = 0.9982$
Limit of detection (ppb)	2.6	1.7	1.8	9.6
RSD(%)				
Migration time	0.3	0.3	0.3	0.3
Peak height	13.8	3.9	6.9	8.5
Corrected area	9.4	3.7	4.8	5.3
Plates	$1.3 \times 10^6$	$8.1 \times 10^5$	$4.9 \times 10^5$	$9.4 \times 10^4$

Packard 3D capillary electrophoresis system equipped with a capillary (50- $\mu$ m inside diameter, 56 cm to the detector, and 64.5 cm total length) thermostated at 20°C. Burning off a 3-mm portion of the polyimide capillary coating formed the detection window.

8. The value of  $k$  was computed for phenanthrene as

marker of the micelle and with the equation  $t_{mc}/(t_r - t_{mc})$ , where  $t_{mc}$  and  $t_r$  are the migration times of the marker and analyte, respectively.

9. The trend of Eq. 2 was not verified for the higher  $k$  values, because accurate determination of  $k$  when values are very high (>100) is difficult. This is be-

cause elution occurs rapidly (peak compression) and no separation occurs without the addition of aqueous-phase modifiers to the BGs.

10. With 2-m-long capillaries and applied voltage at -30 kV, migration times were more than 1 hour.

11. Sweeping enhancement factor = peak height obtained with sweeping/peak height obtained with usual injection (1 or 2 s at 50 millibars). Supplementary material is available at [www.sciencemag.org/feature/data/983374.shl](http://www.sciencemag.org/feature/data/983374.shl).

12. Conditions: injected length of  $S$ , 42 cm; other conditions are the same as in Fig. 2; equation of the line,  $\log(\text{ppb}) = (\text{slope}) \times \log(\text{mAU}) + y$  intercept; calibration concentration range, 10 to 100 ppb; limit of detection, signal/noise ratio = 3; %RSD ( $n = 7$ ).

13. We thank Drs. K. Otsuka and N. Matsubara for support. J.P.Q. is also grateful to the Ministry of Education, Science, Culture, and Sports, Japan (Monbusho) for a Ph.D. scholarship. Supported in part by grants-in-aid for scientific research (nos. 07554040 and 09304071) from Monbusho.

24 June 1998; accepted 16 September 1998

## Increased Vascularization in Mice Overexpressing Angiopoietin-1

Chitra Suri, Joyce McClain, Gavin Thurston, Donald M. McDonald, Hao Zhou, Eben H. Oldmixon, Thomas N. Sato, George D. Yancopoulos\*

The angiopoietins and members of the vascular endothelial growth factor (VEGF) family are the only growth factors thought to be largely specific for vascular endothelial cells. Targeted gene inactivation studies in mice have shown that VEGF is necessary for the early stages of vascular development and that angiopoietin-1 is required for the later stages of vascular remodeling. Here it is shown that transgenic overexpression of angiopoietin-1 in the skin of mice produces larger, more numerous, and more highly branched vessels. These results raise the possibility that angiopoietins can be used, alone or in combination with VEGF, to promote therapeutic angiogenesis.

Vascular development can be divided into an early stage (vasculogenesis) and a later stage (angiogenesis) (1). During vasculogenesis, endothelial cells differentiate, proliferate, and coalesce to form a primitive vascular network. Subsequently, this network is transformed into the mature vasculature through angiogenic remodeling processes that involve the sprouting, branching, pruning, and differential growth of vessels, as well as the recruitment of supporting cells.

Two families of growth factors are thought to be largely specific for the vascular endothelium, because expression of their receptors is mainly restricted to endothelial cells (2, 3). These factors include VEGF and its relatives, which are required for vasculogenesis, and the angiopoietins, which appear to be involved in later stages of vessel growth and remodeling. The inactivation of the gene for VEGF or its receptor (VEGFR2) in mice disrupts vascular development at an early stage when endothelial cells begin to differentiate and proliferate (4-6). When angiopoietin-1 (Ang1) or its receptor (Tie2) is inactivated in mice (7-9), the embryos die from the defects in vascular remodeling that occur subsequent to vascular network formation. A factor related to Ang1 (Ang2) apparently acts as a natural antagonist of Tie2 by blocking receptor activation by Ang1 (10). Consistent with this concept, transgenic overexpression of Ang2 results in embryonic lethality due to vascular defects that are similar to those

occurring in the absence of Ang1 or Tie2 (10).

In vitro studies support the notion that Ang1 and VEGF have distinct and complementary roles; Ang1 is not as effective as VEGF in the induction of endothelial cell proliferation or tubule formation in culture, although it can induce sprouting and branch-like phenomena (3, 11). In addition to such remodeling actions, Ang1 may be required for vessel survival or stabilization (9). However, there is no direct evidence that excess Ang1 can promote angiogenesis and vascular remodeling in vivo.

To determine the effects of localized Ang1 overexpression, we generated transgenic mice that overexpressed the protein in their skin. An expression cassette was constructed in which the *Ang1* cDNA was placed under the control of the keratin 14 (K14) gene promoter and enhancer elements (Fig. 1A), which have been previously used to direct gene expression to the skin (12). In transgenic mice that harbor the K14-*Ang1* cassette, skin tissue contained about 12 times the normal amount of Ang1 mRNA (Fig. 1B). In situ hybridization analysis showed that the transgenic transcript was localized to the basal keratinocyte layer of the epidermis as well as to the keratinocytes that line hair follicles (Fig. 1C).

Transgenic mice overexpressing Ang1 appeared generally healthy, as they gained weight and bred normally. However, the skin of these mice appeared strikingly different from that of the control mice. The newborn transgenic mice had many more large blood vessels in their skin (Fig. 2A). The skin of older transgenic mice was markedly redder than normal and became progressively redder from the ages of 2 weeks to 2 months (Fig. 2, B to D), indicating that transgenic Ang1 continued to have effects during postnatal growth.

Distinctive changes in the microvasculature were evident in whole mount preparations of the skin of adult mice, in which vessels were

C. Suri, J. McClain, H. Zhou, G. D. Yancopoulos, Regeneron Pharmaceuticals, 777 Old Saw Mill River Road, Tarrytown, NY 10591, USA. G. Thurston and D. M. McDonald, Department of Anatomy and Cardiovascular Research Institute, University of California, San Francisco, CA 94143, USA. E. H. Oldmixon, Rogers Imaging, Needham, MA 02192, USA. T. N. Sato, University of Texas, Southwestern Medical Center, Dallas, TX 75235, USA.

\*To whom correspondence should be addressed. E-mail: [gdy@regpha.com](mailto:gdy@regpha.com)

## REPORTS

visualized with fluorescein-labeled dextran (Fig. 3, A and B) or a biotin-labeled lectin (Fig. 3, C and D). Dermal capillaries and venules were more numerous, more highly branched, and (in some cases) enlarged in the skin of transgenic mice. Although the vessels appeared to be rather normal in most skin regions, the skin from the tip of the ear consistently contained prominently enlarged venules that were

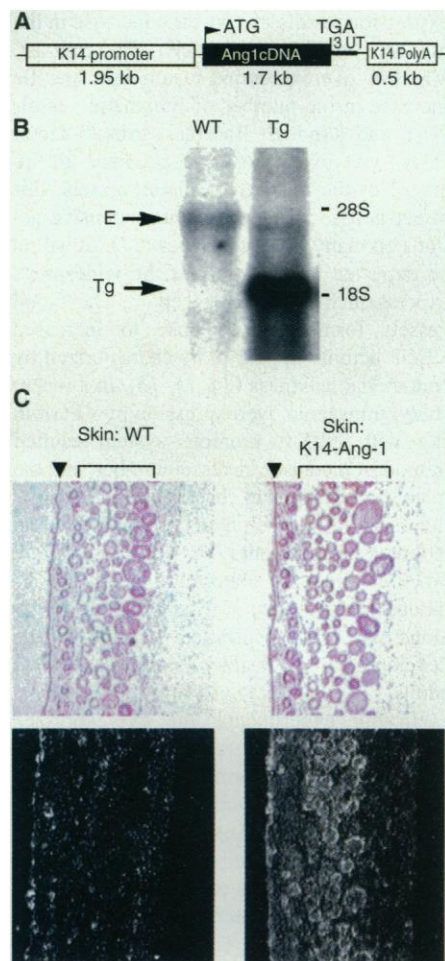


**Fig. 1.** Overexpression of Ang1 in the skin of transgenic mice. (A) The K14-Ang1 expression cassette consisted of 1.7 kb of the mouse *Ang1* cDNA (containing the full coding region), which was cloned into a Bam H1 site between the K14 gene promoter/enhancer and the K14 polyadenylation sequence (12). (B) Northern blot analysis of the total RNA (10  $\mu$ g) isolated from the skin of adult transgenic (Tg) and wild-type (WT) littermates with a probe for Ang1 as described (10). Densitometry was used to determine the relative levels of the transgenic and endogenous Ang1 transcripts (Tg, transgenic Ang1 transcript of  $\sim$ 2.5 kb; E, endogenous Ang1 transcript of  $\sim$ 4.8 kb; positions of 28S and 18S ribosomal RNA are indicated). (C) In situ hybridization analysis of the skin of wild-type and transgenic mice with a probe for Ang1 as described (10). Top panels depict bright-field photomicrographs in which the basal layer of the epidermis (arrow) and hair follicles (bracket) are indicated; bottom panels depict dark-field images after in situ hybridization.

abnormally shaped because of vascular varicosities (Fig. 3D, inset). Such characteristic regional differences in Ang1 action may be due to interactions with other localized angiogenic mediators.

Histological sections of skin, which were

stained immunohistochemically for the endothelial cell-specific marker PECAM (platelet and endothelial cell adhesion molecule), also showed more numerous (Fig. 3, E to H) and enlarged (Fig. 3, I and J) vessels in adult transgenic mice in comparison to their wild-

**Fig. 2.** Overt skin phenotype in newborn and adult Ang1 transgenic mice. (A) Transgenic pups can easily be distinguished from wild-type littermates because of their enlarged surface blood vessels. (B to D) The skin of 2-week-old transgenic mice was only slightly redder than that of wild-type littermates but became increasingly redder as the mice grew older. The transgenic line with the most dramatic phenotype is depicted; a less visible version of the phenotype was evident in other lines, which was consistent with lower expression of the transgenic Ang1 in those lines.

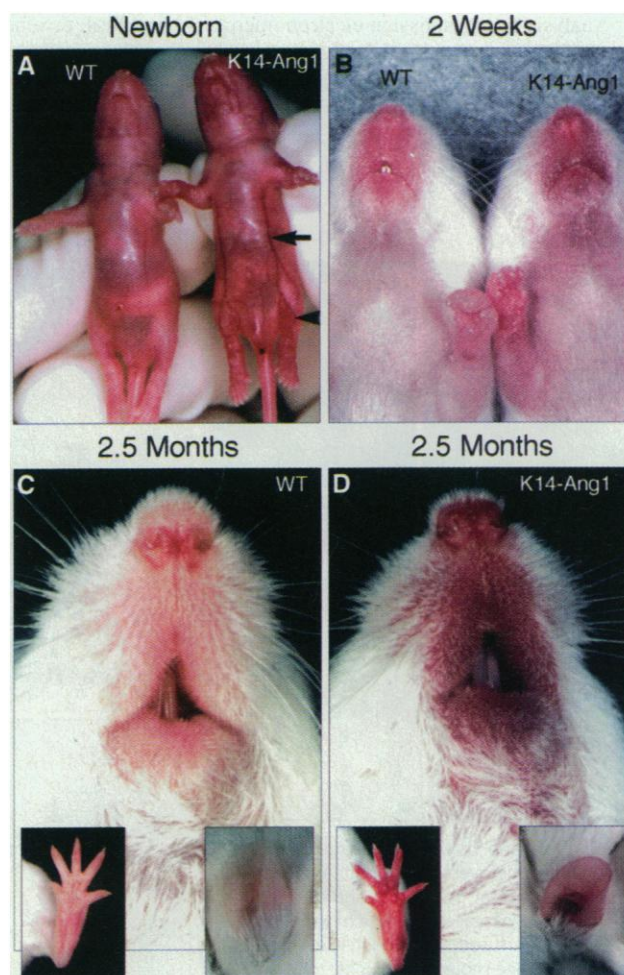


**Table 1.** Comparison of blood vessel length density and shape between transgenic and wild-type mice; quantitation was done on skin samples from four transgenic mice (all from the line that exhibited the most dramatic phenotype) and four control mice, as described (28, 29). The vessel length density was obtained stereologically from the counts of vessel profiles that were observed per unit area of section tissue, and this density represents the total length of vessels per unit volume, as described (28, 29). The vessel profiles were either roughly ellipsoidal (as expected of a section through a cylindrical vessel segment) or Y-shaped (as expected for a section through a vessel bifurcation or branch). The fraction of the branched vessel profiles reflects the number of branched profiles over the total number of vessel profiles. The minimum caliber diameter of the vessel profiles provides a measure of the vessel luminal girth; 367 vessels from the skin of control mice and 966 vessels from the skin of transgenic mice were measured to obtain this data, and a uniform increase in the luminal girth of transgenic vessels was noted across all microvessel sizes. Standard deviations are provided for the vessel density and branched vessel fraction measurements, and probability values ( $P$ ) are provided for all transgenic values. Two-tailed  $t$  tests assuming equal variance in two groups ( $n = 4$ ) were used to determine  $P$  for vessel density and branched vessel fraction, and the two-sample Kolmogorov-Smirnov test was used to compare the minimal caliber diameter data from transgenic versus wild-type tissue of pooled vessels.

Mice	Vessel density (mm/mm <sup>3</sup> )	Fraction of vessel profiles that are branched	Minimum caliber diameter ( $\mu$ m)
Wild type	61.5 $\pm$ 21.8	0.041 $\pm$ 0.003	6.952
Transgenic	124.0 $\pm$ 34.0 ( $P = 0.089$ )	0.220 $\pm$ 0.018 ( $P = 0.00003$ )	9.933 ( $P = 0.0000001$ )

## REPORTS

type littermates, as did three-dimensional reconstructions that were derived from optical sectioning of tissue examined en bloc (Fig. 3, K and L). A quantitative analysis of these sections confirmed that there was a particularly striking increase in vessel branching and further showed that vessel size was uniformly increased in all microvessels (Table 1).

Analysis by transmission electron microscopy (TEM) confirmed that the transgenic vessels exhibited normal cell-cell contacts between endothelial cells and adjacent pericytes and fibroblasts (Fig. 3, M and N). The endothelial cell width was slightly increased

in transgenic vessels, and no evidence of plasma leakage, edema, or erythrocyte extravasation was detected in either the whole mount preparations or in the sections. Thus, the vasculature in the skin of transgenic mice was largely intact and functional as judged by the healthy appearance of the skin and the absence of hemorrhage, edema, ulceration, hair loss, or other skin lesions.

Our results show that overexpression of Ang1 in vivo results in a dramatic increase in the number, size, and branching pattern of blood vessels. The particularly striking increase in branching suggests a key role for

Ang1 in this aspect of angiogenesis, which is consistent with observations indicating that Ang1 can promote sprouting and branchlike phenomena in vitro (11). In addition, suggestions that Ang1 may stabilize endothelial cells (9) raise the possibility that the increased vascularization may also result from decreases in the vessel pruning and regression that normally accompany physiological angiogenesis (13). Ang1 and VEGF (14, 15) are the only factors whose transgenic overexpression results in a specific increase in the number of blood vessels. In contrast, VEGF-C overexpression results in a specific increase in the number of lymphatic vessels (16), and although fibroblast growth factor (FGF) overexpression can produce an increase in the number of blood vessels, this effect is associated with more extensive actions on many other cell types (17), as would be expected on the basis of the widespread expression of the FGF receptor. The blood vessels formed in response to increased VEGF activity appear to be characterized by endothelial leakiness (14, 15, 18). In a recent study, transgenic overexpression of VEGF in skin with the K14 promoter system resulted in modest increases in vessel number, and the mice showed signs of chronic skin inflammation such as vessel hyperpermeability and leukocyte recruitment (19). These results, and other evidence of abnormalities in VEGF-induced vessels (20, 21), suggest that VEGF alone may be an insufficient stimulus for the development of healthy blood vessels in adults.

In our experiments, the overexpressed Ang1 most likely interacts with endogenous angiogenic agents normally present in skin, such as VEGF (22). During embryonic development, VEGF and Ang1 appear to play coordinated and complementary roles (4–10), with VEGF required early in development and Ang1 required later for vascular remodeling and maturation. Thus, in the context of therapeutic angiogenesis (for example, to promote neovascularization of an ischemic heart, the skin, or limb muscles), the best results might be achieved by manipulating both the VEGF and angiopoietin systems so as to not only increase the number of vessels but also to ensure that the new vessels form and function properly.

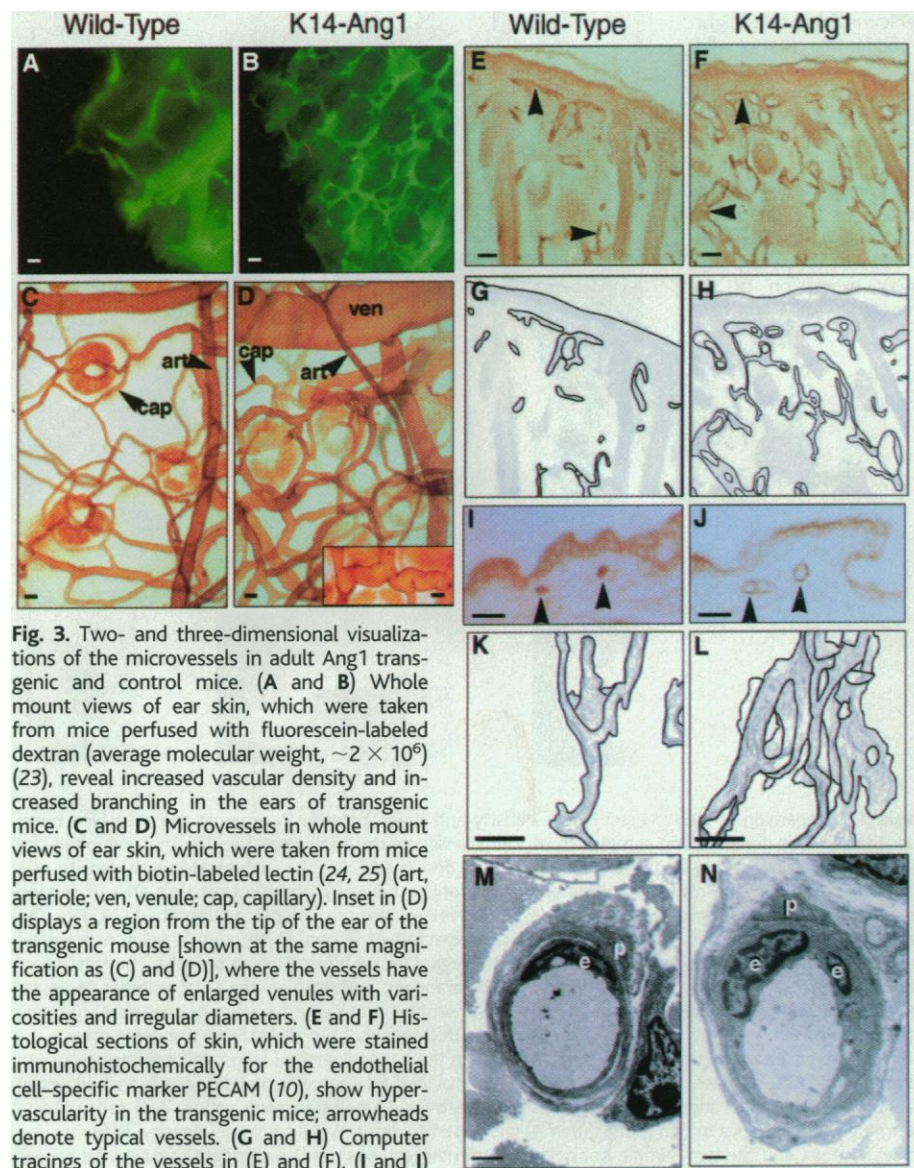


**Fig. 3.** Two- and three-dimensional visualizations of the microvessels in adult Ang1 transgenic and control mice. (A and B) Whole mount views of ear skin, which were taken from mice perfused with fluorescein-labeled dextran (average molecular weight,  $\sim 2 \times 10^6$ ) (23), reveal increased vascular density and increased branching in the ears of transgenic mice. (C and D) Microvessels in whole mount views of ear skin, which were taken from mice perfused with biotin-labeled lectin (24, 25) (art, arteriole; ven, venule; cap, capillary). Inset in (D) displays a region from the tip of the ear of the transgenic mouse [shown at the same magnification as (C) and (D)], where the vessels have the appearance of enlarged venules with varicosities and irregular diameters. (E and F) Histological sections of skin, which were stained immunohistochemically for the endothelial cell-specific marker PECAM (10), show hypervascularity in the transgenic mice; arrowheads denote typical vessels. (G and H) Computer tracings of the vessels in (E) and (F). (I and J) Higher power views illustrating the large vessels in transgenic skin, which (in comparison to the microvessels in control mice) have visible lumens; arrowheads denote vessel cross sections. (K and L) Three-dimensional computer reconstructions of typical vessel patterns in dorsal skin samples that were stained with the fluorescent dye lucifer yellow and examined as a whole by optical sectioning (26, 27). (M and N) Ultrastructural analysis with Zeiss EM10 transmission electron microscopy reveals normal microvessel architecture and cell-cell contacts in transgenics (e, endothelial cell nucleus; p, pericyte cell nucleus). The scale bars represent 25  $\mu\text{m}$ , except in panels (M) and (N), where they represent 1  $\mu\text{m}$ .

### References and Notes

1. W. Risau, *Nature* **386**, 631 (1997).
2. T. Mustonen and K. Alitalo, *J. Cell Biol.* **129**, 895 (1995).
3. S. Davis *et al.*, *Cell* **87**, 1161 (1996).
4. F. Shalaby *et al.*, *Nature* **376**, 62 (1995).
5. P. Carmeliet *et al.*, *ibid.* **380**, 435 (1996).
6. N. Ferrara *et al.*, *ibid.*, p. 439.
7. D. J. Dumont *et al.*, *Genes Dev.* **8**, 1897 (1994).
8. T. N. Sato *et al.*, *Nature* **376**, 70 (1995).
9. C. Suri *et al.*, *Cell* **87**, 1171 (1996).
10. P. C. Maisonpierre *et al.*, *Science* **277**, 55 (1997).
11. T. I. Koblizek, C. Weiss, G. D. Yancopoulos, U. Deutsch, W. Risau, *Curr. Biol.* **8**, 529 (1998).

12. R. Vassar, M. Rosenberg, S. Ross, A. Tyner, E. Fuchs, *Proc. Natl. Acad. Sci. U.S.A.* **86**, 1563 (1989).  
 13. L. E. Benjamin, I. Herno, E. Keshet, *Development* **125**, 1591 (1998).  
 14. N. Okamoto *et al.*, *Am. J. Pathol.* **151**, 281 (1997).  
 15. X. Zeng, S. E. Wert, R. Fereici, K. G. Peters, J. A. Whitsett, *Dev. Dyn.* **211**, 215 (1998).  
 16. M. Jeltsch *et al.*, *Science* **276**, 1423 (1997).  
 17. M. L. Robinson *et al.*, *Development* **121**, 505 (1995).  
 18. C. J. Drake and C. D. Little, *Proc. Natl. Acad. Sci. U.S.A.* **92**, 7657 (1995).  
 19. M. Detmar *et al.*, *J. Invest. Dermatol.* **111**, 1 (1998).  
 20. J. M. Rosenstein, N. Mani, W. F. Silverman, J. M. Krum, *Proc. Natl. Acad. Sci. U.S.A.* **95**, 7086 (1998).  
 21. G. S. Robinson and L. P. Aiello, *Int. Ophthalmol. Clin.* **38**, 89 (1998).  
 22. J. Viac, S. Palacio, D. Schmitt, A. Claudy, *Arch. Dermatol. Res.* **289**, 158 (1997).  
 23. J. A. Nagy *et al.*, *Cancer Res.* **55**, 360 (1995).  
 24. G. Thurston, P. Baluk, A. Hirata, D. McDonald, *Am. J. Physiol.* **271**, H2547 (1996).  
 25. G. Thurston *et al.*, *J. Clin. Invest.* **101**, 1401 (1998).  
 26. E. Oldmixon, H. Brismar, J. Lai, B. Ekstein, R. A. Rogers, *FASEB J.* **8**, A691 (1994).  
 27. K. Takahashi *et al.*, *J. Clin. Invest.* **93**, 2357 (1994).  
 28. E. Weibel, *Practical Methods for Biological Morphometry*, vol. 1 of *Stereological Methods* (Academic Press, New York, 1979), p. 143.  
 29. E. Oldmixon, J. P. Butler, F. G. Hoppin, *J. Appl. Physiol.* **67**, 1930 (1989).  
 30. We thank L. S. Schleifer and P. Roy Vagelos for support; M. Detmar, S. Davis, P. Maisonpierre, and P. Jones for discussions; R. Rogers for confocal microscopy; B. Fowle for electron microscopy; M. Simmons and T. Murphy for technical assistance; C. Murphy and E. Burrows for graphics; and E. Fuchs for the K14 promoter/enhancer construct. D.M.M. and G.T. were supported in part by NIH grants HL-59157 and HL-24136.

3 August 1998; accepted 14 September 1998

# Host-Race Formation in the Common Cuckoo

Karen Marchetti,\* Hiroshi Nakamura, H. Lisle Gibbs

The exploitation of a new host by a parasite may result in host-race formation or speciation. A brood parasitic bird, the common cuckoo, is divided into host races, each characterized by egg mimicry of different host species. Microsatellite DNA markers were used to examine cuckoo mating patterns and host usage in an area where a new host has been recently colonized. Female cuckoos show strong host preferences, but individual males mate with females that lay in the nests of different hosts. Female host specialization may lead to the evolution of sex-linked traits such as egg mimicry, even though gene flow through the male line prevents completion of the speciation process.

Avian brood parasites lay their eggs in the nests of other bird species and raise none of their own young, often greatly reducing the reproductive success of their hosts. Parasitism typically results in the evolution of host discrimination and rejection of unlike eggs which, in turn, selects for improved egg mimicry by the parasite (1, 2). The common cuckoo, *Cuculus canorus*, is divided into different host races, or gentes, each characterized by egg mimicry (1, 2) but showing no differentiation in mitochondrial or nuclear DNA markers (3), which implies rapid host-race evolution. The first step in host-race formation is the exploitation of a new host, followed by adaptation to that host. In central Japan, cuckoos began to exploit the azure-winged magpie (*Cyanopica cyana*) 20 to 30 years ago as a result of expansion of the magpie's breeding range (4–6). Cuckoos also utilize two other hosts in the area: the great reed warbler (*Acrocephalus arundinaceus*) and the bull-headed shrike (*Lanius bucephalus*) (4–7). To investigate the process of host-race formation in this cuckoo

population, we have studied the mating system and patterns of individual host use (8).

To date, the mating system of the cuckoo has been impossible to determine directly because parents do not attend nests and are difficult to catch and mark. We used eight cuckoo-specific microsatellite DNA markers (9) to establish the parentage of 136 chicks collected from known host nests. From these data, we determined cuckoo mating patterns (monogamous, polygamous, or promiscuous) and individual differences in host use (specialist or generalist). We captured and genotyped 83 adult males and 79 adult females. Adult cuckoos were sexed on the basis of behavioral observations (4–6) or by use of a DNA-based sex identification test (10). Examination of variation at the different microsatellite loci enabled us to assign at least one sampled adult as the parent of 84% (114 out of 136) of nestlings sampled with a high degree of confidence ( $P < 0.01$ ) (11). We assigned parentage only if parent or parents and offspring matched unambiguously at eight out of eight microsatellite loci (12).

To determine cuckoo mating patterns, we examined whether adults that produced more than one offspring also mated with more than one individual. The mating system is polygamous, with substantial numbers of both male and female cuckoos having multiple partners (Fig. 1). Previous studies implied that common cuckoos mate multiply (1, 5, 13), and a recent molecular study has shown

polygamous mating in a different cuckoo species (14). There are no demonstrable sex differences in the proportion of individuals that had multiple mates [within years, individuals being included only once, 7 out of 15 males and 3 out of 18 females had more than one mate (Fisher exact test,  $P = 0.13$ )].

To determine patterns of host use (specialist or generalist), we examined whether individual cuckoos that produced more than one offspring had offspring in the nests of more than one host species. Among males and females that were parents to two or more chicks, there were similar numbers of chicks (Fig. 2) ( $n = 92$  chicks in males and 93 in females), but they were distributed differently. Seven of the 19 males but only 2 of the 24 females had offspring in nests of more than one host (Fisher exact test,  $P < 0.05$ ). Thus, male and female cuckoos differ in host specificity, and males are more generalized in

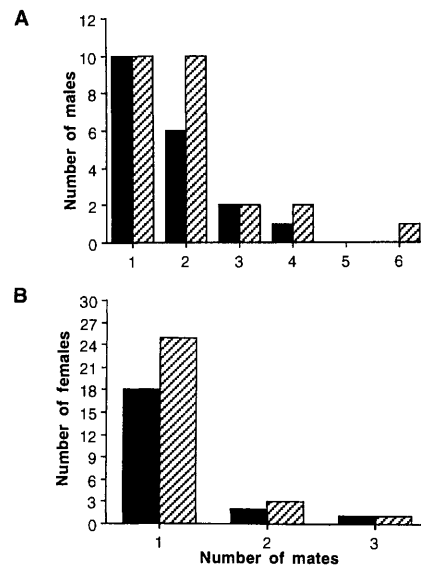


Fig. 1. Number of mates per individual male (A) and female (B) during 1991–1994. Only individuals producing more than one offspring are included. Individuals are tallied across all years combined (hatched bars) as well as separately for each season (black bars). In the latter case, if an individual had two or more offspring in more than 1 year, it was scored separately for each year. Total sample sizes are as follows: males within years, 19; males across years, 25; females within years, 21; females across years, 29.

K. Marchetti and H. L. Gibbs, Department of Biology, McMaster University, 1280 West Main Street, Hamilton, L8S 4K1 Ontario, Canada. H. Nakamura, Department of Biology, Faculty of Education, Shinshu University, Nishinagano, Nagano, 380, Japan.

\*To whom correspondence should be addressed at Department of Biology 0116, University of California, San Diego, La Jolla, CA 92093, USA. E-mail: Marchet@biomail.ucsd.edu